
JOURNAL OF THE AMERICAN CHEMICAL SOCIETY

Synthetic Melittin, Its Enantio, Retro, and Retroenantio Isomers, and Selected Chimeric Analogs: Their Antibacterial, Hemolytic, and Lipid Bilayer Action

Padmaja Juvvadi, Satyanarayana Vunnam, and R. B. Merrifield*

Contribution from The Rockefeller University, 1230 York Avenue, New York, New York 10021

Received December 28, 1995[⊗]

Abstract: Melittin, the principal toxic component of bee venom, is a cationic, amphipathic, linear peptide composed of 26 amino acids, which exhibits unique structural and biological characteristics. It has high antimicrobial activity but also has the very detrimental property of killing eucaryotic cells, as illustrated by the lysis of sheep red cells. Several attempts have been made through synthesis of replacement analogs to advance the molecular understanding of the cause of these effects. We have now synthesized retro melittin, an amphipathic α -helical analog with reversal of sequence and therefore of the positions of charged and apolar residues, notably, the cluster of basic residues Lys²¹-Arg-Lys-Arg²⁴ near the C-terminus which is now located at positions 3–6 near the amino terminus. This peptide retained high antimicrobial activity against a range of test bacteria, but lost much of its hemolytic properties. Modification of the N-terminal positive charge by acetylation did not further alter the antibacterial activity or red cell lysis. The synthetic retroenantio melittin (all-D isomer) and its acetylated derivative both retained full antibacterial activity, but with complete elimination of the hemolytic effect. Therefore, the two effects of melittin have been separated. Melittin and these analogs promote electrical conductivity in lipid bilayers. Circular dichroism measurements showed that all of these peptides—normal, enantio, retro, retroenantio, and their acetylated derivatives—were 80–100% helical in 12–20% hexafluoro-2-propanol, a structure inducing solvent, and they are thought to be helical in lipid bilayers and bacterial membranes. Nonhelical analogs are inactive. It is believed that the helix dipole plays a major part in orienting the peptides in membranes. Active sequences are not unique, but sequence plays a role in peptide conformation and activity. Chirality has virtually no role in the antibacterial activity of normal and retro melittin analogs, which leads to the conclusion that these peptides do not function via a receptor or by enzymatic processing, but by self-aggregation and formation of ion-conducting pores.

Introduction

Cytotoxic amphipathic peptides represent a wide variety of natural components produced by living cells, and are generally basic. Melittin, with a broad antibacterial activity spectrum and very high hemolytic activity, is the major protein component of the venom of the European honey bee, *Apis mellifera*. It is a cationic 26-amino acid peptide, with a C-terminal amide,

which exhibits unique structural characteristics¹ and is one of the best studied peptides. Melittin has a linear sequence and helical amphipathicity, with a basic hydrophilic, highly charged C-terminal segment composed of four adjacent basic amino acids (positions 21 to 24) connected to a predominantly hydrophobic sequence (positions 1 to 20). It has high antimicrobial activity but also has the property of killing eucaryotic

[⊗] Abstract published in *Advance ACS Abstracts*, September 15, 1996.

(1) Habermann, E.; Jentsch, J. *Hoppe-Seyler's Z. Physiol. Chem.* **1967**, *348*, 37–50.

N per g) (Peptide International, Louisville, KY), either manually by our most effective methods or on an Applied Biosystems model 430A synthesizer. Protected amino acids were obtained from Peninsula Laboratories (Belmont, CA). The couplings with dicyclohexylcarbodiimide in dichloromethane, or preformed symmetrical anhydrides in dimethylformamide (DMF), or HOBt esters in dimethylformamide, were monitored by the quantitative ninhydrin method.²⁹ The *tert*-butoxycarbonyl (Boc) group was used for temporary N^o-protection of amino acids, and more acid stable groups (2-chlorobenzyloxy carbonyl for Lys and formyl for Trp) were used for side chain protection. The N^o-Boc group was removed at each cycle and from the completed peptide-resin by 50% trifluoroacetic acid (TFA) in methylene chloride. The Nⁱⁿ-formyl protecting group on tryptophan was removed by reacting twice for 1 min each with 50% piperidine in DMF and the peptide was cleaved from the resin using either high or low/high HF procedures.³⁰

Peptides were purified by a two-step procedure: gel filtration on a 2.4 × 90 cm column of Sephadex G-25 (Pharmacia LKB, Piscataway, NJ), eluted with 1 M AcOH at 45 mL/h, followed by reverse phase preparative HPLC on a 2.2 × 25 cm, Vydac C18 column (218TP, 15–20 μm, 300 Å pores, The Separations Group, Hesperia, CA) using a linear gradient of 10–60% acetonitrile in water both containing 0.05% TFA at a rate of 20 mL/min. The eluent was monitored at 220 nm on a Kratos Spectroflow 757 absorbance detector. The main peak was assessed for homogeneity by analytical HPLC with a reverse phase column, 0.46 × 25 cm, Vydac C18, 5 μm, 300 Å and the composition determined by amino acid analysis. Hydrolysis of free peptides was done with 6 N HCl in evacuated, sealed tubes at 110 °C, 18 h.³¹ The molecular weight of the purified peptide was determined by electrospray mass spectrometry.³² Agreement with values calculated from most abundant isotopes was always within 0.5 mu.

Antibacterial Plate Assays. Thin agar plates were prepared with 6 mL of rich medium containing 1–4 × 10⁵ colony-forming units of the respective log-phase test bacteria.³³ Wells of 3-mm diameter were punched in the plates and for each peptide and each test bacterium, 3-μL aliquots of a series of peptide dilutions were placed in the wells. The concentration of each peptide was determined from its absorbance at 280 nm ($\epsilon = 5.6 \times 10^3 \text{ cm}^{-1} \text{ M}^{-1}$). Plates were incubated overnight at 38 °C, the diameters of the zones of inhibition were measured to ±0.1 mm under a microscope, and the lethal concentration (LC), defined as the lowest concentration that completely inhibits growth, was calculated as described³³ in which the square of the zone diameter vs log of the peptide concentration was fit to a straight line and extrapolated to the concentration giving no zone of growth inhibition. The statistical analysis of the data was done according to “goodness of fit”. The regression analysis was performed using Microsoft Excel programme. To determine the fit of a set of experimental observations with calculated data the χ^2 test is used, which is based on a calculation of the quantity χ^2 defined as

$$\chi^2 = \sum_{i=1}^n [(\text{obsd value})_i - (\text{calcd value})_i]^2 / (\text{calcd value})_i$$

The larger the χ^2 value, the larger is the disagreement between the observed and calculated values or the smaller probability of fit. If $\chi^2 = 0$ then the observed value exactly fits the calculated ones. To determine if these results occurred by chance the probability *P* is obtained by calculating the number of degrees of freedom and χ^2 from the experimental data. Calculations have been made^{34,35} of the

(29) Sarin, V. K.; Kent, S. B. H.; Tam, J. P.; Merrifield, R. B. *Anal. Biochem.* **1981**, *117*, 147–157.

(30) Tam, J. P.; Heath, W. F.; Merrifield, R. B. *J. Am. Chem. Soc.* **1983**, *105*, 6442–6445.

(31) Crestfield, A. M.; Moore, S.; Stein, W. H. *J. Biol. Chem.* **1963**, *238*, 622–627.

(32) Chowdhury, S. K.; Katta, V.; Chait, B. T. *Rapid Commun. Mass Spectrometry* **1990**, *4*, 81–87.

(33) Hultmark, D.; Engstrom, A.; Andersson, K.; Steiner, H.; Bennich, H.; Boman, H. G. *EMBO J.* **1983**, *2*, 571–576.

(34) Mood, A. M.; Graybill, F. A. *Introduction to the theory of statistics*, 2nd ed.; McGraw-Hill Book Co.; New York, 1963.

(35) Wilson, E. B. *An introduction to scientific research*; McGraw-Hill Book Co.; New York, 1952.

probability that the actual measurements match the expected distribution. If the *P* value lies between 0.1 and 0.9, the observed distribution is considered to follow the calculated distribution. The bioassay results reported here are the ones which showed the probability values in the range of 0.1 and 0.9. Replicate assays done on different days usually agree within 20%.

Hemolysis Assays. (1) Plate assay: The antibacterial plate assay was adapted to an erythrocyte lysis assay. The plates were made from 5.4 mL of an aqueous solution containing 1% agarose and 0.9% NaCl and 0.6 mL of a 10% suspension of sheep erythrocytes in Alsever's solution. The dilution series of the peptide was placed in the wells. After incubation at 38 °C for 20 h, the diameters of the clear zones were measured and LC values calculated.³³ The statistical analysis of the data was done as described for the antibacterial assay data.

(2) Colorimetric assay: The hemolytic assays²⁰ were determined using rat or sheep red blood cells. A 0.5% suspension of washed red blood cells was diluted in phosphate buffered saline (PBS: 150 mM NaCl + 7.5 mM sodium phosphate) at pH 7.2. An RBC suspension (50 μL) at a density of 2 × 10⁷ cells/mL in PBS was then added to 50 μL of eight 2-fold serially diluted concentrations of peptide and incubated for 45 min at 37 °C. The RBC were pelleted and the supernatant diluted 1/100 in 0.05 M Tris-HCl, pH 7.9, for hemoglobin determination at 415 nm. A 100% hemolysis sample was prepared by treating an RBC suspension with triton. Supernatant from an RBC suspension incubated without peptide served as a baseline hemolysis control.

Conductivity in Planar Lipid Bilayers. The experimental setup and procedure for the electrical measurements on planar bilayers were similar to those described in detail.^{36,37} The entire cell assembly was washed three times, sequentially with 30% methanol in chloroform, ethanol, and then water. The electrolyte was unbuffered 1.0 M NaCl at 25 ± 1 °C. The cell was fixed in the cell holder, and KCl-saturated calomel electrodes (Ingold, Wilmington, MA) connected the aqueous compartments to the measuring circuit. The membrane potential was determined as the potential difference between the two electrodes at opposite sides of the lipid bilayer. The voltage source was manually variable. Planar bilayers were formed from a mixture of lipid solution 90% dioleoyl phosphocholine and 10% phosphatidylserine (10 mg/mL in decane) (both from Avanti Polar Lipids, Pelham, AL) on a pretreated hole (0.5–0.8-mm diameter) with a fine brush or a pipet in a Teflon septum separating two half cells. On standing for a few minutes the solvent diffused out and the lipid self organized into a black lipid bilayer. Bilayer formation was followed by an increase in capacitance. The rear compartment (trans) was held at ground and voltage was applied to the front (cis) compartment. Current measurements were performed with a home-built current-to-voltage converter (based on a Zeltex 133 operational amplifier) with a feed back resistance of 10⁹ ohms and a feed back capacitance between 10 and 300 pF, yielding cutoff frequencies between 3 and 100 Hz. The amplifier output was recorded on a chart recorder (series 4900 super scribe, Houston Instruments, Austin, TX) and was observed simultaneously on a Biomation 802 transient recorder (Gould, Santa Clara, CA).

For the experiments to resolve channel conductances we used a Axopatch-1B (Axon instruments) integrating patch clamp to apply the membrane potential across the measure current through the membrane. The setup is described in detail elsewhere.³⁷

The membrane thickness was estimated from its measured capacitance using the relation $d = \epsilon A/C$, where *d* is the thickness of the bilayer in Å, ϵ is the dielectric constant of the lipid, *A* is the area of bilayer in mm², and *C* is the capacitance in faraday. The basic conductance of the bilayer was recorded for at least 15 min. The conductance did not exceed 0.02 nS and no channel activity was observed. The peptides at 30–4000 ng/mL concentrations were dissolved in water and added to the cis compartment at 0 mV, and an equal volume of water was added to the trans compartment. They were allowed to equilibrate for at least 30 min. A potential of –10 to 20 mV was applied until the pore activity was observed, and then the voltage was changed from negative to positive values. The voltage was applied for enough time (~10 min) to collect signals from pores opening and closing.

(36) Drain, C. M.; Christensen, B.; Mauzerall, D. *Proc. Natl. Acad. Sci. U.S.A.* **1989**, *86*, 6959–6962.

(37) Andersen, O. S. *Biophys. J.* **1983**, *41*, 119–133.

Table 1. Percentages of α -Helix, β -Sheet, and Random Coil in Retro and Retroenantiomeric Melittin Analogs^a

peptide amide	0% HFIP			4% HFIP			8% HFIP			12% HFIP			16% HFIP			20% HFIP		
	α	β	<i>r</i>	α	β	<i>r</i>	α	β	<i>r</i>	α	β	<i>r</i>	α	β	<i>r</i>	α	β	<i>r</i>
L-melittin	9	57	0	70	0	30	60	17	23	86	14	0	84	2	13	88	12	0
D-melittin	10	58	38	77	15	8	87	8	0	87	8	5	89	7	4	89	11	0
retro melittin	6	60	35	18	56	26	47	36	16	81	17	2	96	4	0	100	0	0
Ac-retro melittin	4	64	32	20	59	21	54	30	16	89	10	0	100	0	0	100	0	0
retroenantiomeric melittin	0	96	4	11	84	5	26	70	4	70	21	10	82	15	3	85	15	0
Ac-retroenantiomeric melittin	13	55	31	55	27	18	93	7	0	100	0	0	100	0	0	100	0	0

^a Calculated from the circular dichroism measurements by the Provencher program.³⁸

Circular Dichroism Analyses. CD spectra were recorded on an Aviv 62DS spectropolarimeter. Peptides (final concentration of 25 μ M) were dissolved in 2.5 mM sodium phosphate buffer, pH 7.4, containing 0–20% (v/v) hexafluoro-2-propanol (HFIP). Five consecutive 250–190 nm scans were made in a 1 mm path length cell at 22–25 °C. The data were averaged and analyzed by the method of Provencher³⁸ which determines the percentage of α -helix, β -sheet, β -turn, and random coil by a linear combination of the CD spectra of 16 proteins whose secondary structures are known from X-ray crystallography.³⁹ The statistical analysis given by this program indicates when the fit is acceptable. In order to estimate the quality of the secondary structure obtained a parameter termed “probability to reject” was also considered. This parameter was ideally between 0.1 and 0.9 indicating the goodness of fit.

Energy Minimization Dynamics. Tertiary structure diagrams were made with INSIGHTII (Biosym Technologies, San Diego, CA) and displayed on a Silicon Graphics workstation. Minimization and dynamics were performed on melittin and retro melittin starting from a random extended conformation *in vacuo* using Discovery and INSIGHTII programs. Dynamics simulations (6000K) and energy minimization sets were performed. Each set contains 10 000 dynamic time steps followed by 1000 steepest descent minimization iterations. Various intermediate conformations were examined and analyzed for possible conformations that might explain the differences in the activities of the two peptides.

Results

The peptides reported here were synthesized by solid-phase methods and purified by chromatography on Sephadex and on a preparative reverse phase C-18 silica column, and then found to be >97% homogeneous on an analytical HPLC in a different solvent system. No racemization was expected by this synthetic method. The peptide compositions were confirmed by amino acid analysis and mass spectrometry, so we are confident of their quality. The primary sequences of the peptides are shown in Figure 1.

Melittin and retro melittin and their enantiomers have the same net charge and hydrophobic moment, though the direction of hydrophobic moment and the charge topology are different. These sequences are highly amphipathic when folded in an α -helix as illustrated by Edmundson wheels. The four positively charged lysine and arginine side chains of the melittin C-terminus extend away from the backbone of the helix and are therefore projected to all sides³⁹ and the entire circumference of the helix is charged in the C-terminal region. These residues were shown by CD and Raman experiments^{11,13} not to be in the helical region of melittin. The ¹H-NMR studies of melittin bound to micelles also show that melittin forms a helix on interaction with membranes.⁴⁰

Chou-Fasman calculations predict a strong helical potential ($\langle P \rangle$ 1.2) for residues 1–10 and 1.1 for residues 13–20 in melittin and 1.1 for 7–13 and 1.2 for residues 17–26 of retro

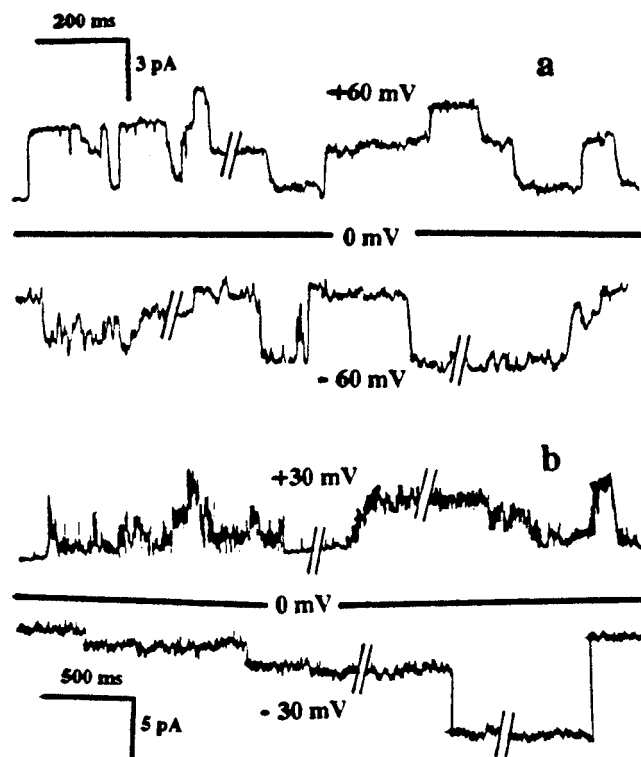


Figure 2. Bilayer conductivity induced by (a) melittin and (b) retroenantiomeric melittin. Multiple state pore is formed with several conducting states before it closes. These traces show a long lifetime of the conducting states.

melittin. Circular dichroism of the L and D melittins and their retro peptides revealed mainly a β conformation in phosphate buffer at pH 7.2, while the α -helical conformation increased with increasing concentration of HFIP, a structure-inducing solvent (Table 1). Melittins and their retro analogs were found to be 80–100% α -helical at 12–20% of HFIP. L-Melittin, with *all-L* amino acids, is a right-handed helix. Its enantiomer, with *all-D* residues, is a left-handed helix. L-Melittin is a mirror image of D-melittin as supported by CD spectra.

The L and D enantiomers of melittin and retro melittin show pore conductance and an increase in macroscopic conductance with applied voltage. Melittin did not show any channel formation at <10 mV applied potential, but showed an exponentially increased multistate pore activity up to 60 mV. Multiple pore conductance levels observed (Figure 2a) are likely due to the interaction of melittin with lipid bilayer. These discrete steps are probably because of small open channels within the bilayer. Reversing the voltage source to negative on the peptide side made it more noisy but we could resolve the multistate pores even at –60 mV. Figure 2a shows that the channels remain open in different levels for a long (1–2 s) duration of time. The low level of conductance appears to be more stable and is open for a longer time (2.5 pA current passing through the open channel for 1.2 s). In general, structural

(38) Provencher, S. W.; Glockner, J. *Biochemistry* **1981**, *20*, 33–37.

(39) Terwilliger, T. C.; Weissman, L.; Eisenberg, D. *Biophys. J.* **1982**, *37*, 353–361.

(40) Inagaki, F.; Shimada, I.; Kawaguchi, K.; Hirano, M.; Terasawa, I.; Ikura, T.; Go, N. *Biochemistry* **1989**, *28*, 5985–5991.

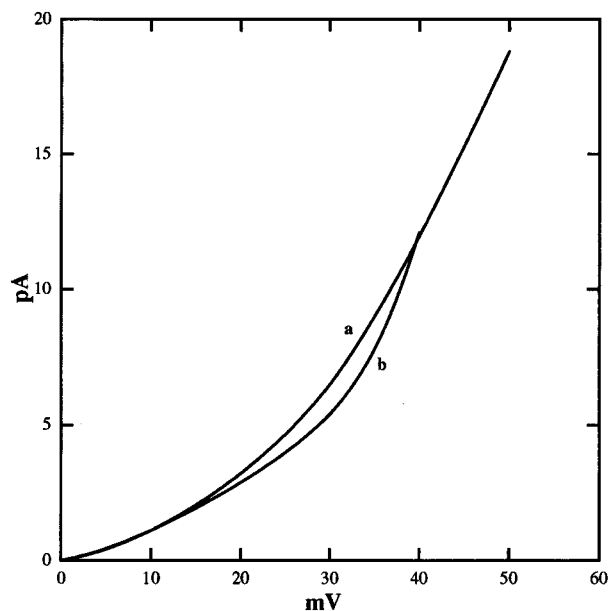


Figure 3. Current–voltage curves of (a) melittin and (b) retroenantio melittin treated planar bilayer. Both peptides were added only to the cis compartment with a final concentration of $0.12 \mu\text{M}$.

Table 2. Lethal and Lysis Concentrations (μM) for Melittin Analogs^a

peptide amide	size	D21	OT 97	Bs 11	Sp 1	Sac 1	SRC
L-melittin	26	0.8	3.0	0.2	0.5	0.2	4–8
Ac-L-melittin	26	1.34	4.4	0.94	0.73	3.94	1–2
D-melittin	26	1.0	2.0	0.4	0.9	0.1	2–3
Ac-D-melittin	26	1.4	3.4	0.5	0.4	3.7	2–3
retro melittin	26	1.04	1.07	0.39	0.31	0.4	38
Ac-retro melittin	26	0.9	0.96	0.19	0.24	0.38	42
retroenantio melittin	26	0.57	1.62	0.36	0.6	2.11	>400
Ac-retroenantio melittin	26	0.55	1.49	0.52	0.95	0.4	>400

^a Lethal concentrations calculated from inhibition zones on agarose plates seeded with the respective organisms: D21 = *E. coli*; OT97 = *P. aeruginosa*; Bs11 = *B. subtilis*; Sp1 = *Strep. Pyogenes*; Sac1 = *Staph. aureus*; SRC = sheep red cells.

channels are associated with discrete steps of increased conductance corresponding to the opening and closing process.

Retro melittin also showed burst-like current fluctuations and a dramatic increase when a “threshold” voltage was reached, which in this case was in the range of ± 26 to ± 40 mV. We could resolve the pore-state fluctuations at ± 30 mV (Figure 2b). The long-lived channels in this case were between 0.5 and 0.8 s, with an average current of 2–3 pA.

Similar behavior was noticed with the D isomers. The L and D enantiomers thus interact with lipid bilayer in a similar way and show voltage-dependent pore fluctuations. An exponential increase in conductance was observed with all these analogs when the voltage was applied. The I/V plot of melittin and retroenantio melittin are presented in Figure 3.

The antibacterial and hemolytic activities of the analogs were measured by inhibition-zone assays on agarose plates, from which the lethal concentrations were calculated (Table 2). Retro melittin with either a free or N^α-acetylated amino terminus was observed to be as active as melittin against one Gram-negative and three Gram-positive bacterial strains, but both analogs were approximately three times more active against *Pseudomonas aeruginosa*. This is somewhat beyond our normal experimental error. The assay data suggest that neither the free amine nor N^α-acetyl amine in retro melittin has any noticeable effect on the activity against bacteria.

Against *Staphylococcus aureus*, melittin (LC $0.2 \mu\text{M}$) and acetyl retroenantio melittin (LC $0.4 \mu\text{M}$) were both very active,

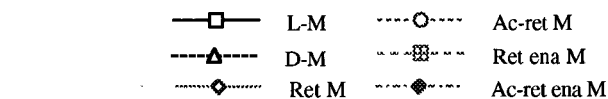
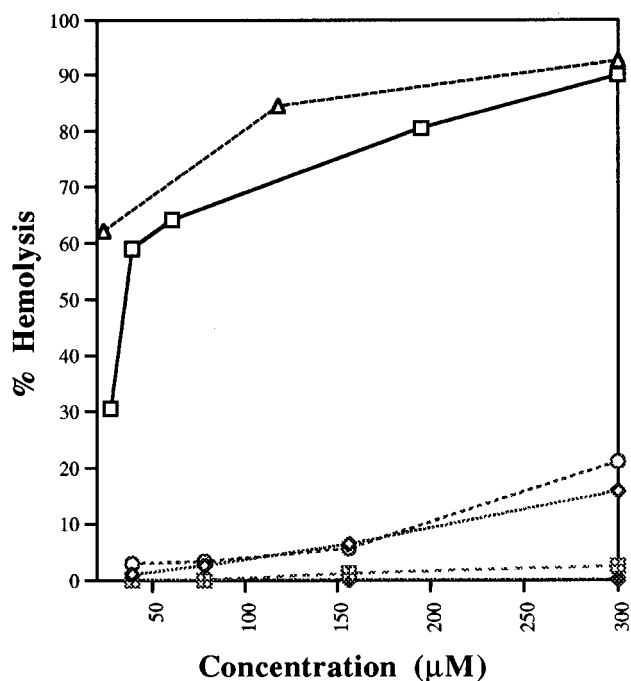


Figure 4. Colorimetric hemolysis assay.

but retroenantio melittin (LC $2.1 \mu\text{M}$) was 5 to 10 times less active. The latter number was reproduced twice, but the explanation is not clear. With this one exception, the L and D enantiomeric pairs of melittin, retro melittin, and Ac-retro melittin were all essentially equally active for all five organisms, showing that chirality is not an important feature for antibacterial activity. This leads to a strong and important conclusion to be discussed later.

The hemolytic activities of each peptide were determined by using two different procedures on both sheep and rat red blood cells and the results were compared. L-Melittin and D-melittin were equally effective and were very lytic toward red cells in both assays; 4–8 μM LC in the plate assay (Table 2) and 60% lysis at $50 \mu\text{M}$ in the colorimetric assay (Figure 4). In contrast, retro melittin had an LC of $38 \mu\text{M}$ and only 5% lysis was produced by $50 \mu\text{M}$ (colorimetric assay). Acetylation of the free α amine of retro melittin had no effect on its hemolytic activity in the plate assay (LC = $42 \mu\text{M}$) or colorimetric assay (5% at $50 \mu\text{M}$).

Retroenantio melittin and N^α-acetyl retroenantio melittin were non-lytic by both assays up to $300 \mu\text{M}$. At extremely high concentration in the $5000 \mu\text{M}$ range a maximum of 20–30% lysis was observed with these peptides.

To further examine the effects of amphipathicity, hydrophobicity, charge, and helical dipole, we have synthesized hybrid analogs of melittin and cecropin A and some melittin analogs containing rearranged sequences, and measured their antibacterial activity and red cell lysis (Table 3). For example, the two terminal segments of melittin were reversed [M(16–26)M(1–13) and M(21–26)M(1–20)] and activity against all five bacterial strains was retained, but red cell lysis was reduced or eliminated. M(20–1)M(21–26) retained the hydrophobic and basic segments in their parent positions but inverted the 1–20 sequence to give the retro sequence 20–1. This gave nearly full antibacterial and lytic activity. An analog containing an

Table 3. Lethal and Lysis Concentrations (μM) for Melittin and Their Cecropin Hybrid Analogs^a

peptide	size	D21	OT 97	Bs 11	Sp 1	Sac 1	SRC
L-M(16–26)M(1–13) NH ₂	24	0.7	8.0	0.7	1.0	10	>200
L-M(21–26)M(1–20) NH ₂	26	0.49	0.92	0.30	0.28	0.54	22.85
L-M(20–1)M(21–26) NH ₂	26	1.56	3.09	0.65	1.11	1.71	5–6
L-M(26–21)M(1–20) NH ₂	26	0.38	1.48	0.24	0.46	0.19	16.58
L-CA(1–8)M(21–26) NH ₂	14	38.16	>300	40.4	6.44	11.58	>300
L-CA(1–8)M(19–26) NH ₂	16	6.8	>200	5.91	3.0	83.9	>300

^a Lethal concentrations calculated from inhibition zones on agarose plates seeded with the respective organisms: D21 = *E. coli*; OT97 = *P. aeruginosa*; Bs11 = *B. subtilis*; Sp1 = *Strep. Pyogenes*; Sac1 = *Staph. aureus*; SRC = sheep red cells.

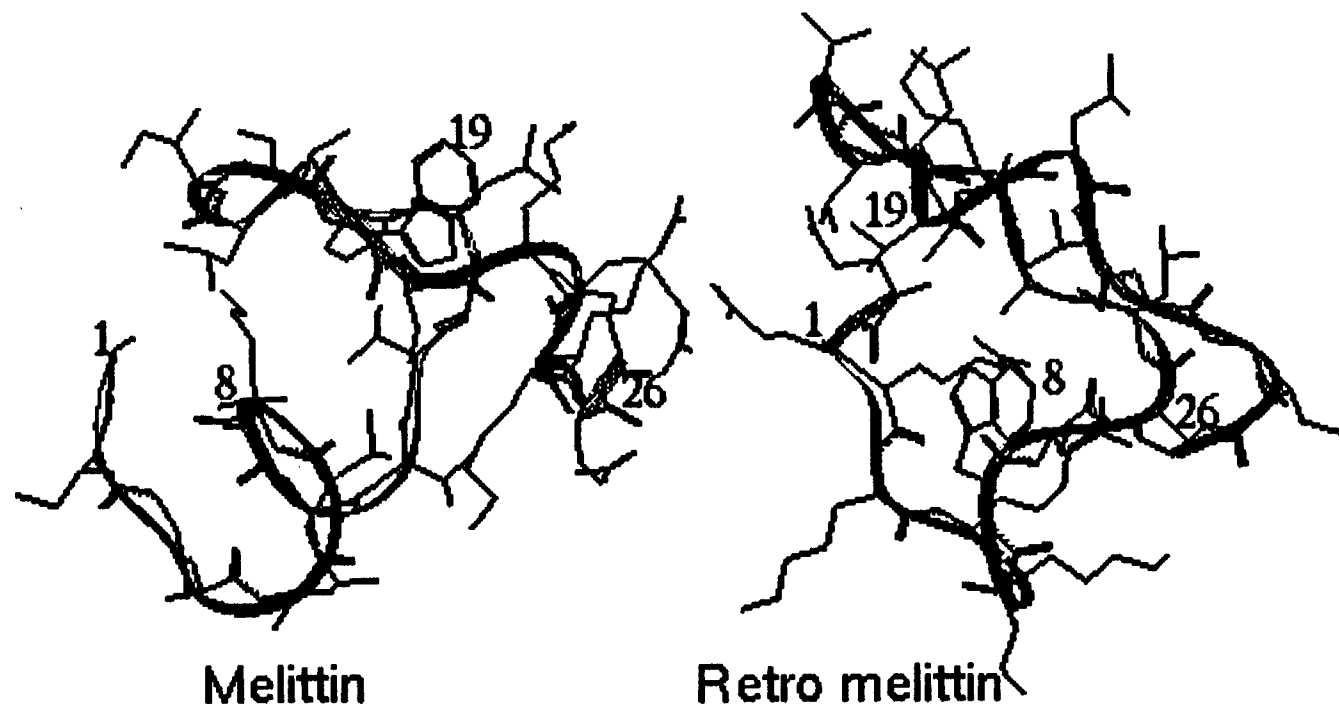


Figure 5. Tertiary structures of melittin and retro melittin, obtained by energy minimization procedures. Trp¹⁹ of melittin is relatively exposed, whereas Trp⁸ of retro melittin is occluded by the peptide backbone and nearby side chains. Examination of all the orientations led to the same conclusion.

unrelated amphipathic 1–20 sequence and the melittin 21–26 sequence was shown⁴¹ to retain antibacterial and anti red-cell activity.

Several hybrids of melittin and cecropin A were also assayed (Table 3). For example, the chimeric derivative CA(1–8)M(21–26)NH₂ retains the basic 1–8 sequence of cecropin at the N-terminus, containing Trp², and the strongly charged basic sequence of melittin at the C-terminus. Another analog, CA(1–8)M(19–26)NH₂, also contained a Trp¹⁹ adjacent to the basic residues 21–24. These analogs were inactive against both bacteria and red blood cells and did not conduct current in lipid bilayers.

Since tryptophan is a conserved residue in all natural cecropins (residues 1 or 2) and is also found in melittin (residue 19) and in retro melittin (residue 8), its presence and location may be a critical factor in determining the differences in the lytic action of these peptides. A minimum energy structure of retro melittin was calculated as described in the Experimental Section. The data after 53 000 dynamic time steps (Figure 5) suggest that Trp⁸ is internal in the folded peptide and therefore shielded from interactions with the cell. In contrast, the corresponding Trp¹⁹ residue of melittin is more exposed, which may contribute to its lytic properties.

Discussion

This work has been designed to add new quantitative data for our studies on the molecular mechanism by which melittin

and other members of this class of peptides exert their antibacterial and hemolytic effects. It relies primarily on synthetic organic chemistry.

To interpret the antibacterial and hemolytic assay data obtained from L-melittin, D-melittin, L-retro melittin, D-retro melittin, and their N^α-acetyl derivatives a table was constructed relating the expected activities with a series of assumptions about which structural features are important for high activity (Table 4). Comparison with the observed pattern of activities of the analogs against five test organisms and erythrocytes (Table 2) allowed us to deduce which structures are significant for the killing of each cell type. It was observed that for four of the bacterial strains all eight analogs gave high lethal activity. This result corresponds only with assumptions 1 and 2, meaning that sequence or helical dipole direction (amide bond direction) could be important for activity but not both at the same time as predicted for assumption 4. All analogs also gave high activity against *Staph. aureus* except acetyl L-melittin and acetyl D-melittin. This does not correspond with any of the assumptions of Table 4. It suggests that this organism is more sensitive to these antibiotics if they contain a free α -amino group. The results with erythrocytes do fit structural requirement 4, which assumes that both sequence and helical dipole direction must be the same as in L-melittin. The fit is relatively good although some (about 10%) lysis did occur with L-retro melittin and its acetyl derivative. The data show clearly that (with the exception of *Staph. aureus*) antibacterial and hemolytic activities do not

Table 4. Predicted Activity of Melittin Analogs as a Function of Required Structure^a

assumed structural requirements	predicted activity ^b						
	L-M	D-M	L-retro	D-retro	acetyl L-M	acetyl L-retro	acetyl D-retro
1. sequence	+	+	+	+	+	+	+
2. dipole direction	+	+	+	+	+	+	+
3. chirality	+	-	+	-	+	+	-
4. sequence + dipole	+	+	-	-	+	-	-
5. sequence + chirality	+	-	-	-	+	-	-
6. dipole + chirality	+	-	+	-	+	+	-
7. sequence + dipole + chirality	+	-	-	-	+	-	-

^a Assumes active structure is helical. ^b + means activity approximately equivalent to L-melittin. - means no or low activity.

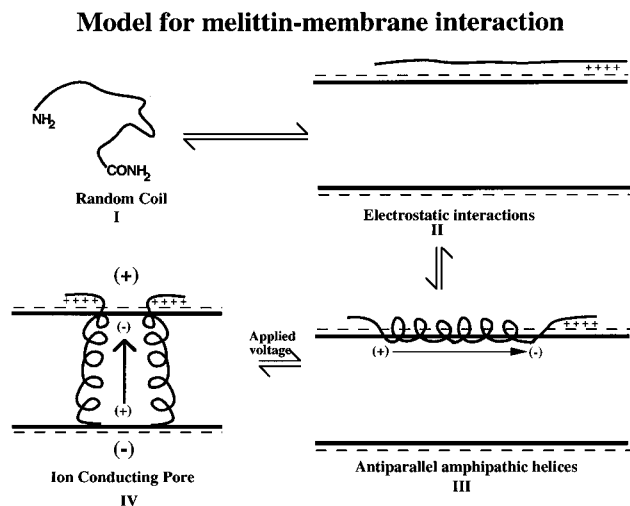


Figure 6. A suggested mechanism for electrical conductivity through a membrane induced by melittin.

depend on the presence of a free α amino group since all four N^{α} -acetyl peptides gave the same response as the corresponding peptides bearing a free amino group.

It is specifically shown here that chirality does not play a role in activity because the L and D melittins and L and D retro melittins are equally active against a range of bacterial species. These results agree with our previous data on the cecropins and some of their hybrids.^{41,42} They are qualitatively different, however, from many results on peptide hormones,^{43a,b} which are known to transduce their effects through receptors. In all cases the *all*-D enantiomers of the hormones were inactive. The observations that antibacterial activity is essentially independent of peptide chirality are interpreted to mean that the lethal activity is not due to close specific binding interaction between the chiral peptides and various chiral components of bacteria such as receptors, carriers, enzymes, or lipids. Rather, it is a result of self-aggregation of the peptides themselves when in a hydrophobic environment to form pore structures within the cell membrane.

We have demonstrated ion channels (pores) in planar lipid bilayers for melittin and retro melittin and their *all*-D isomers. Earlier, cecropins⁴⁴ were also shown to form ion-channels.

We believe that the proposed mechanism for melittin (outlined in Figure 6) best explains its actions, and a related one was earlier proposed for cecropins. It is based in part on the cecropin work and in part on the earlier melittin experiments from the

laboratories of Tosteson,⁴⁵ Hol,⁴⁶ Vogel,¹² Boheim and Jung,⁴⁷ Durell,⁴⁸ Balam,⁴⁹ DeGrado,⁴¹ Houghten,¹⁷ and others, and on a review by Dempsey.²¹ Thus, (I) the basic peptide monomer in dilute aqueous solution in a random conformation is thought (II) to bind electrostatically to the anionic phospholipid surface of the lipid bilayer to form a layer of peptide monomers and (III) a rearrangement occurs which brings the hydrophilic surface into contact with the polar head groups of the lipid and the hydrophobic residues into contact with the apolar hydrocarbon chains of the fatty acids. This induces the amphipathic helical conformation, with a large helical dipole. The helices would be aligned antiparallel to minimize their energy. Finally, (IV) under an applied voltage gradient a conformational rearrangement occurs in which the helical segments of dimers insert through the membrane with the negative end of the dipole (the C-terminus) pointing toward the positive electrode and the helices aligned parallel. The peptides then aggregate into helical bundles (probably four or more), which are amphipathic, with the hydrophilic surfaces in the interior of a water-filled pore and the hydrophobic surface facing the apolar hydrocarbon chains. This process would avoid energy expenditure required to desolvate and re-solvate the charged surface.⁴⁸ The charges of the multiple dipoles would repel one another enough to form an ion-channel that can open and close to give the observed conductivity pulses without disruption of the membrane.

We think a similar mechanism holds for the bacterial cell which has a positive (outside) membrane potential. These peptides are known^{50a,b} to decrease the proton gradient, stop ATP and protein synthesis, and result in cell death. Strong evidence for the pore theory in bacteria was provided by Cociancich et al.⁵¹ when they showed that the cell could be induced by peptide to pass K^+ , ATP^- , and other ions without loss of the membrane potential.

We realize that other mechanistic views have been proposed. They have been well-reviewed by Boman.⁵² They generally picture the antibiotic forming a monolayer^{53,54,55} on the surface of the cell membrane. The peptide then causes lysis of the

(45) Tosteson, M. T.; Alvarez, O.; Hubbell, W.; Bieganski, R. M.; Attenbach, C.; Caporale, L. H.; Levy, J. J.; Nutt, R. F.; Rosenblatt, M.; Tosteson, D. C. *Biophys. J.* **1990**, *58*, 1367–1375.

(46) (a) Hol, W. G. J.; Van Duijnen, P. T.; Berendsen, H. J. C. *Nature* **1978**, *273*, 443–446. (b) Hol, W. G. J.; Halie, L. M.; Sander, C. *Nature* **1981**, *294*, 532–536.

(47) Boheim, G.; Hanke, W.; Jung, G. *Biophys. Struct. Mech.* **1983**, *39*, 181–191.

(48) Durell, S. R.; Raghunathan, G.; Guy, H. R. *Biophys. J.* **1992**, *63*, 1623–1631.

(49) Mathew, M. K.; Balam, P. *FEBS Lett.* **1983**, *157*, 1–5.

(50) (a) Okada, M.; Natori, S. *Biochem. J.* **1984**, *222*, 119–124. (b) Okada, M.; Natori, S. *Biochem. J.* **1985**, *229*, 453–458.

(51) Cociancich, S.; Ghazi, A.; Hetru, C.; Hoffmann, J. A.; Letellier, L. *J. Biol. Chem.* **1993**, *268*, 19239–19245.

(52) Boman, H. G. *Annu. Rev. Immunol.* **1995**, *13*, 61–92.

(53) Steiner, H.; Andreu, D.; Merrifield, R. B. *Biochem. Biophys. Acta* **1988**, *939*, 260–266.

(54) Pouny, Y.; Rapaport, D.; Mor, A.; Nicolas, P.; Shai, Y. *Biochemistry* **1992**, *31*, 12416–12423.

(41) Wade, D.; Boman, A.; Wahlin, B.; Drain, C. M.; Andreu, D.; Boman, H. G.; Merrifield, R. B. *Proc. Natl. Acad. Sci. U.S.A.* **1990**, *87*, 4761–4765.

(42) Merrifield, E. L.; Mitchell, S. A.; Ubach, J.; Boman, H. G.; Andreu, D.; Merrifield, R. B. *Int. J. Peptide Protein Res.* **1995**, *46*, 214–220.

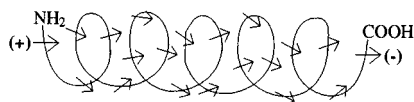
(43) (a) Stewart, J. M.; Woolley, D. W. *Nature* **1965**, *206*, 619–620. (b) Flouret, G.; Duvigneaud, V. *J. Am. Chem. Soc.* **1965**, *87*, 3775–3776.

(44) Christensen, B.; Fink, J.; Merrifield, R. B.; Mauzerall, D. *Proc. Natl. Acad. Sci. U.S.A.* **1988**, *85*, 5072–5076.

Table 5. Effects of Sequence, Helix Dipole, and Charge on Killing and Lysis

Peptide amide	Dipole ^a and charges ^b	LC E. coli (μM)	LC Red cell Lysis (μM)
1. M(1-26)	—————>++++	0.8	4
2. M(20-1)M(21-26)	—————>++++	1.56	8
3. Retro M(26-1)	++++—————>	1	38
4. M(26-21)M(1-20)	++++—————>	0.4	17
5. M(16-26)M(1-13)	—————++++>	0.7	>200
6. CA(1-37)	+++++—————>	0.2	>200
7. CA(1-13)M(1-13)	+++++—————>	0.5	>200
8. CA(25-37)CA(1-22)	—————++++>	10	>200
9. CA(1-10)M(18-26)	+++++—————>++++	1	>500
10. CA(1-8)M(19-26)	+++++—————>++++	7	>300
11. CA(25-37)M(15-26)	—————>++++	11	>900

^a The arrows point toward the negative end of the helical dipole. ^b The basic segment of melittin is indicated by + + + +. The basic segment of cecropin is indicated by + + + + +.

**Figure 7.** The helical dipole.

bacterial cell by a “wedge mechanism”^{16,56} or in other unspecified ways. This view is supported by correlating the lethal concentration with the amount of peptide required to form a monolayer on the cell surface.⁵³ Raman spectra¹² and solid-state NMR⁵⁷ have shown that some peptides align at the membrane perpendicular to the surface while others are primarily parallel to the surface. The latter orientation is also deduced from fluorescence measurements.⁵⁸ We think a small fraction of the peptides could rearrange to form pores without detection by these methods.

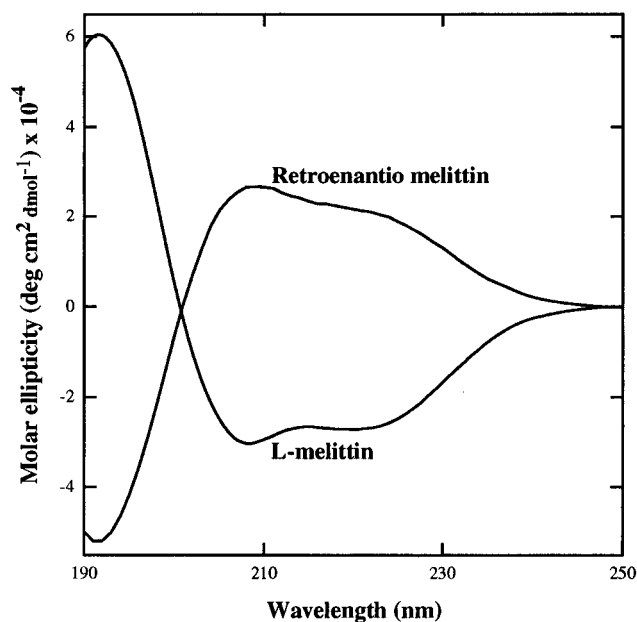
A retro peptide can have the same sequence of side chains as the parent peptide if it is viewed in the C to N direction. However, the amide bonds will be inverted, i.e. —NHCO— rather than the normal —CONH— bond of a conventional peptide structure. Inversion of the amide changes the hydrogen bonding pattern and in particular it changes the helical dipole. In an amide bond the negative pole of the —C=O dipole is on the more electronegative oxygen atom and for the —N—H it is on nitrogen, and both point in the same direction. In an α -helix the amide dipoles all point in the same direction and are nearly parallel and are therefore additive^{46,49} with the negative pole toward the —COOH end of the peptide (Figure 7). The effect can equal roughly one-half of an electrostatic unit at each end of the molecule⁴⁶ and for a long helix this may be approximately 60 kcal/mol.⁴⁹ In melittin the helical dipole is from Gly¹ toward the basic KRKRQQ,²⁶ whereas in retro melittin it will point away from the basic residues toward residue 1 (melittin numbering). We believe that the primary factor in the alignment of peptides across membranes is the helical dipole. The sequence need not be precisely conserved, but it must provide an amphipathic helical conformation for the passage of ions and the killing of susceptible bacteria to occur. It is beneficial if it also provides for a bend in the helical regions. Note that

(55) Gazit, E.; Boman, A.; Boman, H. G.; Shai, Y. *Biochemistry* **1995**, *34*, 11479–11488.

(56) Batenburg, A. M.; De Kruijff, B. *Biosci. Rep.* **1988**, *8*, 299–307.

(57) Bechinger, B.; Zasloff, M.; Opella, S. J. *Protein Science* **1993**, *2*, 2077–2084.

(58) Gazit, E.; Lee, W.-J.; Brey, P. T.; Shai, Y. *Biochemistry* **1994**, *33*, 10681–10692.

**Figure 8.** Circular dichroism spectra of melittin and retroenantio melittin. Experimental conditions: solvent, 2.5 mM phosphate buffer, 20% HFIP pH 7.4, peptide concentration 2.5 μM, temperature 25 °C, number of scans 5, Aviv 62DS spectropolarimeter.

if a given sequence has a potential to be helical its retro sequence will also have a potential to be helical. The CD data (Table 1) show that to be true for melittin and retro melittin. The CD spectra are similar because the peptides have the same amino acid composition but are not identical because they have inverted sequences. For the same reason the spectra of melittin and retroenantio melittin are not exact mirror images (Figure 8).

The principal difference between cecropins and melittin is that the latter is very lytic toward eucaryotic cells, whereas cecropins are not. This has been related to the lipid composition of the cell membranes, especially to the presence of high levels of cholesterol in eucaryotic cells and its absence in bacterial membranes.⁵⁹ We find that both L and D melittin lyse red cells at ~4 μM but that *all*-L retro melittin and its *N*^α-acetyl derivative are about an order of magnitude less active than melittin. Retroenantio melittin (the *all*-D retro analog) and its *N*^α-acetyl

(59) Jackson, M.; Mantsch, H. H.; Spencer, J. H. *Biochemistry* **1992**, *31*, 7289–7293.

derivative were more than 100-fold less lytic by the plate assay and more than 1000-fold less lytic by the colorimetric assay. Thus the reversed sequence, in which the four strongly basic residues (KRKR) are in the amino terminal region and the more hydrophobic residues are in the carboxyl terminal region, does not strongly promote red cell lysis (1 to 3 orders less than L- or D-melittin). It is interesting to note that the negative end of the helix dipole of melittin points toward this basic cluster, whereas it points away in the case of the retro derivatives. This is a significant effect that may be related to the lowered hemolytic activity of the retro derivatives. If the helical dipole is the dominant factor in aligning the peptides across the membrane and the basic $-K^{21}RKRQQ^{26}-NH_2$ is not in the helix^{11,12} but is in contact with the hydrophilic head groups of the phospholipid membrane, then melittin would be oriented so that the amphipathic α -helix, residues Gly¹-Ile²⁰ (+dipole-), aggregates into pores that span the membrane. Retro melittin would also form pores that span the membrane; however, they would be formed from residues Ile²⁰-Gly¹ (+dipole-) (melittin numbering) and the KRKRQQ sequence would be in the interior of the cell. For the red cell this is apparently disfavored.

From these data we tentatively concluded that red cell lysis depends on a particular sequence with normal peptide bonds and with the helix dipole pointing toward the C-terminal basic segment. This reasoning has now been further tested and refined. Table 5 shows the antibacterial and lytic activity of a series of rearranged sequences of melittin and cecropin. The activities were analyzed in terms of the direction of the helical dipole, the location of the basic region of the peptide, and the composition and sequence of the nonbasic segments. Most of these analogs were antibacterially active, but had low or no lytic effect on red cells. Those peptides containing the basic residues at the amino terminus (**3**, **4**, **6**, **7**) were non-lytic or of reduced activity. Those with the basic region located centrally (**5**, **8**) or with basic segments at both ends (**9**, **10**) were also non-lytic. Melittin (**1**), with the basic KRKR segment at the carboxyl end

and the dipole of the remaining amphipathic helix (residues 1–20) pointing toward the C-terminus, was strongly lytic. It was then shown, however, that the normal sequence of melittin did not have to be conserved. When the non-basic 1–20 segment was replaced by a retro sequence 20–1 (**2**), the strong lytic property was maintained. This result was expected because the inverted sequence has the same amino acid composition, nearly the same helical potential, and a similar dipole strength and direction relative to the normal sequence.

When the nonbasic segment was the cecropin A (residues 25–37) sequence no lysis was observed,¹⁴ showing that all random sequences are not adequate. It remains to be determined the effect of membrane composition on susceptibility of bacteria and red cells to killing and lysis by melittin and its analogs.

In summary, we have been able to separate the antibacterial activity of melittin from its killing of eucaryotic cells. Thus, analogs of melittin have been designed and synthesized that are highly lethal toward a range of test bacteria but do not lyse red cells and are much more stable toward enzymatic inactivation than melittin itself. The structural requirements for activity have been studied and a mechanism is proposed, involving pore formation in membranes, that accounts for the observed data.

Acknowledgment. We thank the U.S. Public Health Service (Grant No. DK 01260) for financial support, Professor Brian Chait (Director of the Mass Spectrometric Biotechnology Research Resource of The Rockefeller University) for the Mass Spectral analysis, Anthony Popowicz (Assistant Director, Computing Services of The Rockefeller University) for help with the computational analysis and modeling, and Professor David Mauzerall and Professor Olaf S. Andersen for consultation on conductivity across lipid bilayers and for the use of their equipment.

JA9542911